

Electron-electron interactions in the conductivity of graphene

A. A. Kozikov¹, A. K. Savchenko¹, and B. N. Narozhny²

¹*School of Physics, University of Exeter, EX4 4QL, U.K. and*

²*Institut für Theorie der Kondensierten Materie, Karlsruher Institut für Technologie, 76128 Karlsruhe, Germany*

We investigate the effect of electron-electron interaction on the low-temperature conductivity of graphene. The quantum correction due to electron-electron interaction is separated from that due to weak localization. We show that in graphene the electron-electron interaction correction is more sensitive to the character of disorder than in the 2D systems studied earlier, so that a new temperature regime of interaction can be observed.

PACS numbers:

The classical (Drude) conductivity is determined by electron scattering by impurities and phonons. The quantum (wave) nature of electrons can be seen as corrections to the classical conductivity that are dependent on temperature [1, 2]. This understanding, which was developed a few decades ago, stimulated a new field of condensed matter physics: mesoscopics. The quantum corrections have been studied in different 2D systems and have two distinct origins: interference of electron waves scattered by impurities (weak localization, WL) [1, 2] and electron-electron interaction (EEI) [2].

In graphene, a monolayer of carbon atoms, WL was predicted [3, 4] to exhibit a distinct difference to the usual case: it is sensitive not only to inelastic (phase breaking) scattering, but also to a number of elastic scattering mechanisms. This was confirmed experimentally [5, 6].

Effects of EEI on the conductivity of graphene have not been studied in experiment. Theoretically, it was shown [7] that in the so-called ‘ballistic’ regime, $k_B T \tau_p > 1$ (where τ_p is the momentum relaxation time), the EEI correction in graphene is expected to be different from that in semiconductor 2D systems [8, 9]: due to the chirality of charge carriers EEI is sensitive to the range of the scattering impurity potential. In the ballistic regime the conductivity correction is caused by coherent backscattering of carriers, but in graphene the backscattering is suppressed [10] and can only occur due to atomically sharp defects. In addition, the ballistic regime in graphene can be realized at relatively high temperatures ($T > 50$ K) where the study of the EEI effect is complicated by the need to separate it from strong effects of electron-phonon scattering on the classical conductivity.

In the ‘diffusive’ regime, $k_B T \tau_p < 1$, interacting electrons scatter on multiple impurities (small-angle scattering), and hence the suppression of backscattering should not change the EEI effect, resulting in the conventional Altshuler-Aronov correction [2]:

$$\delta\sigma^{EEI}(T) = -A \frac{e^2}{2\pi^2\hbar} \ln \frac{\hbar}{k_B T \tau_p}, \quad (1)$$

where the strength of interaction A reflects the symmetry of electron states. Although electron-phonon scattering

is less important in this (low-temperature) regime, one still has to separate the correction due to EEI from that due to WL [4],

$$\delta\sigma^{WL}(T) = -\frac{e^2}{2\pi^2\hbar} \left[\ln(1 + 2\tau_\varphi(T)/\tau_i) - 2 \ln \left(\frac{\tau_\varphi(T)/\tau_p}{1 + \tau_\varphi(T)/\tau_i + \tau_\varphi(T)/\tau_*} \right) \right], \quad (2)$$

where τ_φ is the (inelastic) dephasing time, τ_i is the elastic time of inter-valley scattering and τ_* is the elastic time describing intra-valley suppression of quantum interference (by topological defects and ‘trigonal’ warping of the energy spectrum [4]).

In this work we study the EEI effect on the conductivity of graphene in the diffusive regime. To separate the corrections due to EEI and WL, we combine measurements of $\sigma(T)$ with studies of magnetoresistance (MR). We show that in graphene not only WL but also the EEI correction is different from that in non-chiral 2D systems, insofar as it is affected by both elastic times, τ_i and τ_* .

Three samples (S1, S2 and S3) are deposited by the conventional method of mechanical exfoliation of graphite on Si/SiO₂ substrates [11]. Six-terminal devices with Hall-bar geometry and Cr/Au contacts are made using electron-beam lithography. The samples are annealed in vacuum at a temperature of 140°C before cooling down. Quantum Hall effect measurements were performed to verify that the samples are monolayers [11]. Sample parameters are shown in Table 1.

Figure 1 shows the resistivity ρ as a function of the gate voltage for the three samples. The bars indicate three regions of the gate voltage where $\rho(T)$ was measured in all samples: $V_g = 3, 16$ and 36 V with respect to the Dirac point.

Figure 2a shows $\rho(T)$ in sample S1 in the temperature range $T = 5 - 200$ K. The increase of the resistivity at high temperatures is ascribed to the effects of phonon scattering on the classical conductivity [12, 13], while $\rho(T)$ at low temperatures can be attributed to the quantum corrections. The dashed lines show the expected resistivity

Region	S1			S2	S3
	μ	τ_i	τ_*	μ	μ
I	17500	14	0.45	9300	12500
II	11500	3	0.3	5400	11000
III	9700	1	0.35	4500	9500

TABLE I: Electron mobility (in $\text{cm}^2\text{V}^{-1}\text{s}^{-1}$) for three regions of the carrier density in samples S1, S2 and S3. Characteristic scattering times (in ps) are also shown for sample S1.

due to phonon scattering [14]:

$$\rho_{ph}(T) = \left(\frac{\hbar}{e^2}\right) \frac{\pi^2 D_a^2 k_B T}{2h^2 \rho_s v_{ph}^2 v_F^2}, \quad (3)$$

where D_a is the deformation potential constant, $\rho_s = 7.6 \times 10^{-7} \text{ kg m}^{-2}$ is the density of graphene, $v_{ph} = 2 \times 10^4 \text{ m s}^{-1}$ is the speed of sound, and $v_F = 10^6 \text{ m s}^{-1}$ is the Fermi velocity of carriers. We use the value of $D_a = 18 \text{ eV}$ as determined from the analysis of the temperature dependence of the classical conductivity [13].

One can see that in region I the phonon contribution to ρ is negligibly small, while in regions II and III it becomes comparable to the experimental dependence $\rho(T)$ and should be taken into account: we have subtracted the phonon effect in regions II and III. The temperature range is limited to 50 K in order to rule out other types of phonons, which can contribute significantly at higher temperatures [12, 13]. The resulting temperature dependence due to the quantum effects is shown for all regions in Fig. 2b as $\Delta\sigma(T) = \sigma(T) - \sigma(T_0)$, where T_0 is the lowest studied temperature, $\sigma(T) = [\rho(T) - \rho_{ph}(T)]^{-1}$.

The separation of the quantum corrections due to EEI and WL has been performed by two methods. (1) For samples S1 and S3 an additional set of experiments was performed on the low-field perpendicular magnetoresistance, in order to determine the characteristic times $\tau_\varphi(T)$, τ_i and τ_* following the method in [5, 6]. These are then used to determine the WL correction in the temperature dependence of the conductivity according to Eq.(2) and subtract it. (2) In sample S2, the EEI correction has been isolated by suppressing the WL by a perpendicular magnetic field which is still too small to affect the EEI correction [1]. Both methods lead to close results for the magnitude of the EEI correction in the studied samples.

The solid line in Fig. 2b shows the WL correction to the conductivity, $\Delta\delta\sigma^{WL}(T) = \delta\sigma^{WL}(T) - \delta\sigma^{WL}(T_0)$, found from the analysis of the magnetoresistance using method (1). The solid lines show clearly that in regions I and II there is a transition from weak localisation (an increase of $\Delta\sigma(T)$ with increasing T) to antilocalisation (a decrease of $\Delta\sigma(T)$). The transition temperatures of $\sim 10 \text{ K}$ in region I and $\sim 25 \text{ K}$ in region II are in agreement with the range of temperatures in [6] where the transition from WL to WAL was observed at similar carrier

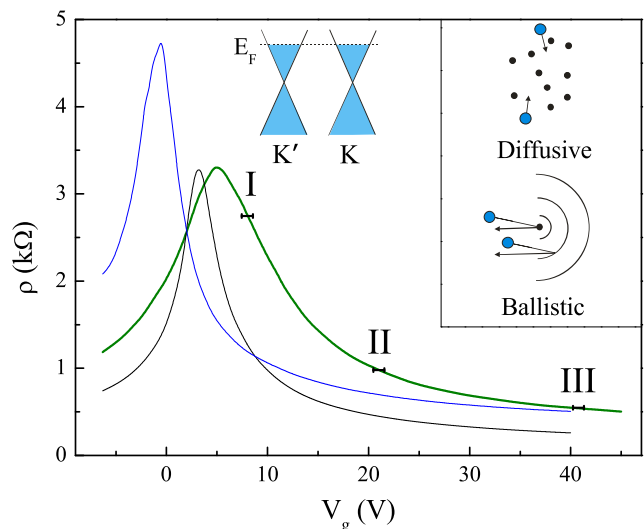


FIG. 1: (Color online). The gate voltage dependence of the resistivity for samples S1 (black), S2 (green) and S3 (blue). The bars (shown for S2) indicate three studied regions. Insets: graphene band structure with two valleys, and a schematic illustration of the regimes of interaction between two electrons that are scattered by impurities.

densities as the change of the sign of MR. One can see that the two types of quantum correction (WL and EEI) are of similar magnitude and therefore there is a clear need to separate them.

Figure 3a shows the temperature dependence of the resistivity of sample S2 (where method (2) is used) in the temperature range 0.25 - 40 K. The phonon contribution, Eq.(3), shown by the dashed lines was subtracted in regions II and III. The results converted into conductivity are shown in Fig. 3b for different magnetic fields. One can see that with increasing B there is a decrease in the slope of the temperature dependence (due to suppression of WL) until further increase of B does not change $\Delta\sigma(T)$. This is a signature that the WL correction has been suppressed while the EEI correction is not affected yet by magnetic field.

Indeed, the suppression of WL is expected at fields which are much larger than the so-called ‘transport’ field $B_{tr} = \hbar/2e l_p^2$, where l_p is the mean free path [15]. For sample S2 the values of B_{tr} are 120, 70 and 45 mT for regions I, II and III, respectively, and therefore it is not surprising that the WL appears to be suppressed at $B = 1 \text{ T}$, Fig. 3b. On the contrary, the effect of the magnetic field on the EEI correction is due to the Zeeman splitting of the triplet ‘channel’ and is expected to be seen when the condition $g^* \mu_B B > 1$ is satisfied [2], where g^* is the effective Landé g -factor, μ_B is the Bohr magneton. With the g -factor in graphene ~ 2 [16], the value of the Zeeman splitting at $B = 1 \text{ T}$ is smaller than $k_B T$ at temperatures above 1 K.

The extracted EEI correction is shown for samples S1

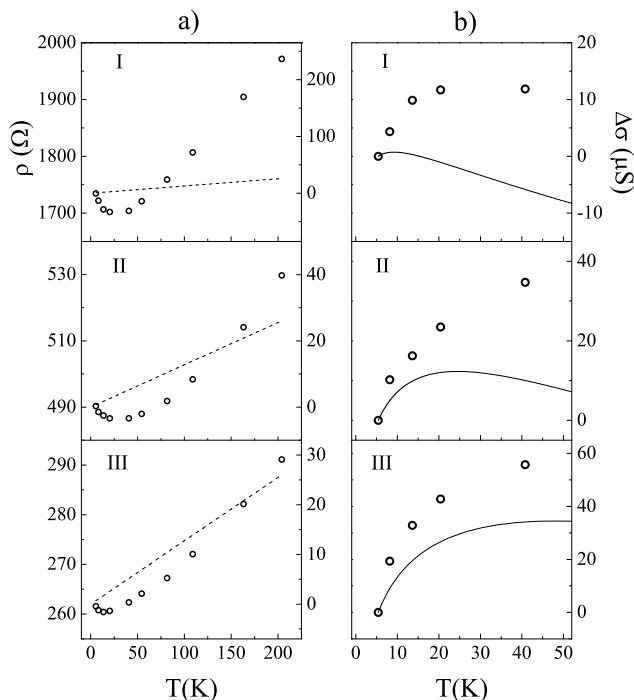


FIG. 2: (a) The resistivity as a function of temperature for sample S1 for three regions of carrier density. The dashed line is the acoustic phonon contribution calculated using Eq.(3) (the right-hand side axis). (b) The conductivity after the phonon contribution has been subtracted. Solid lines show the WL correction found from Eq.(2).

and S2 in Fig. 4, where we also add the result for sample S3 in region I. The extracted correction has indeed the expected logarithmic dependence, Eq.(1), with close values of the coefficient A for all three regions in the studied samples: $A = 0.5 - 0.8$.

The theory [2] distinguishes between the contributions to the interaction correction, Eq.(1), from different eigenstates of the total spin of two interacting electrons. Such states are commonly referred to as ‘channels’. Thus in a simple 2D system (such as in GaAs) the coefficient A takes the form $A = 1 + 3(1 - \ln(1 + F_0^\sigma)/F_0^\sigma)$. Here the unity represents the contribution of the singlet (or charge) channel. If all spin directions are equivalent, the three components of the triplet give identical contributions characterized by the Fermi liquid constant F_0^σ which depends on the carrier density. These contributions are reflected in the second term.

Breaking the spin-rotation symmetry results in suppression of the triplet channel contributions [2, 9]. For example, Zeeman splitting of the spin states in a magnetic field leads to suppression of the contribution of two components of the triplet (those correspond to the non-zero projection of the total spin onto the direction of B -field).

In two-valley 2D systems (e.g., in Si-MOSFETs [17])

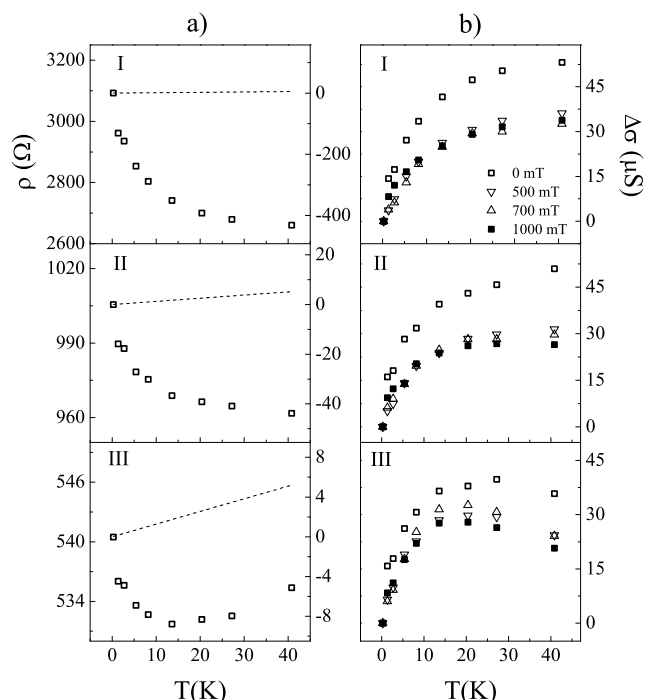


FIG. 3: (a) The resistivity as a function of temperature for sample S2, shown for three regions. The dashed line is the acoustic phonon contribution calculated using Eq.(3) (the right-hand side axis). (b) The conductivity $\Delta\sigma(T) = \sigma(T) - \sigma(T_0)$ at different magnetic fields (the contribution of acoustic phonons has been subtracted).

the situation is more complicated. In the absence of inter-valley scattering, the valley index $v = \pm$ is a good quantum number. In this case the overall number of channels is 16 (due to four components of spin states and four of valley states), and the coefficient A becomes $A = 1 + 15(1 - \ln(1 + F_0^\sigma)/F_0^\sigma)$. This result applies in the presence of weak inter-valley scattering, $k_B T \gg \hbar/\tau_i$, i.e. when the typical electron energy is larger than the characteristic energy of inter-valley scattering. At low temperatures, $k_B T \ll \hbar/\tau_i$, the valleys are mixed and A has the same form as in the single-valley case.

In graphene the effect of the valley degeneracy is governed by two scattering times, τ_i and τ_* [4]. In the EEI correction the inter-valley scattering time τ_i plays a role similar to that in Si-MOSFET, while the effect of the intra-valley time τ_* is similar to the effect of the Zeeman splitting on the spin triplet: \hbar/τ_* represents the ‘decay rate’ of the diffusons in the two ‘valley triplet’ components [18].

As in our experiment $\tau_* < \tau_i$ (Table I), an intermediate temperature regime of the EEI correction becomes possible: $\hbar/\tau_i < k_B T < \hbar/\tau_i + \hbar/\tau_*$. Here in addition to the singlet only one triplet mode of valley states contributes to EEI (the other two are suppressed). Using the values of τ_i and τ_* found from the magnetoresistance, one

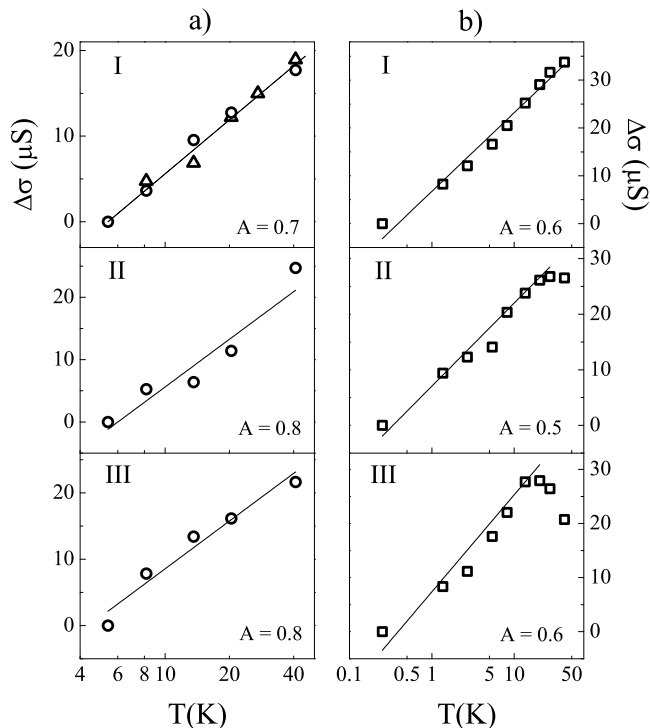


FIG. 4: (a) The electron-electron interaction correction to the conductivity for sample S1 (filled circles) and S3 (empty circles) obtained by subtraction of the WL correction. (b) The electron-electron interaction correction to the conductivity for sample S2 at $B = 1000$ mT obtained by suppression of the WL correction. Solid lines are fits to Eq.(1).

can see that it is this regime that is realized in the experiment. We conclude that there are overall 8 channels contributing to the EEI correction, and therefore A in Eq.(1) takes the form

$$A = 4 [1 + 7 (1 - \ln(1 + F_0^\sigma)/F_0^\sigma)] . \quad (4)$$

(We are using here a common assumption that all channels except for the singlet are described by the same Fermi-liquid parameter.)

An essential difference from Si-MOSFETs is the additional factor of 4 in Eq.(4) appearing due to renormalization of the current vertices by disorder [4, 18, 19]. Using Eq.(4) and the experimental values of A , Fig. 4, we find the values of F_0^σ to be between -0.2 and -0.21. This result appears to be in surprisingly good agreement with the theoretical analysis [20] of the Fermi liquid parameter F_0^σ in graphene for the studied carrier densities $n = (0.2 - 3) \times 10^{12} \text{ cm}^{-2}$.

In summary, we show that electron-electron interaction plays an important role in the low-temperature con-

ductivity of carriers in graphene. We are able to separate the correction due to EEI from that due to WL and show that, due to the linear dispersion relation, the EEI correction in graphene has a different form compared with other 2D systems. It has been found that the chirality of carriers makes it possible for a new temperature regime to be observed, where the magnitude of the EEI correction is affected not only by inter-valley but also by intra-valley elastic scattering.

We are grateful to V. I. Fal'ko, A. D. Mirlin and E. McCann for useful discussions and to R. V. Gorbachev and F. V. Tikhonenko for support in fabricating samples.

-
- [1] G. Bergman, Phys. Rep. **107**, 1 (1984).
 - [2] B. L. Altshuler and A. G. Aronov, *Electron-Electron Interactions in Disordered Systems*, edited by A. L. Efros and M. Pollak (North-Holland, Amsterdam, 1985).
 - [3] H. Suzuura and T. Ando, Phys. Rev. Lett. **89**, 266603 (2002).
 - [4] E. McCann *et al.*, Phys. Rev. Lett. **97**, 146805 (2006).
 - [5] F. V. Tikhonenko *et al.*, Phys. Rev. Lett. **100**, 056802 (2008).
 - [6] F. V. Tikhonenko *et al.*, Phys. Rev. Lett. **103**, 226801 (2009).
 - [7] V. V. Cheianov and V. I. Fal'ko, Phys. Rev. Lett. **97**, 226801 (2006).
 - [8] G. Zala, B. N. Narozhny, and I. L. Aleiner, Phys. Rev. B **64**, 214204 (2002); Y. Y. Proskuryakov *et al.*, Phys. Rev. Lett. **89**, 076406 (2002); A. A. Shashkin *et al.*, Phys. Rev. B **66**, 073303 (2002).
 - [9] S. A. Vitkalov *et al.*, Phys. Rev. B **67**, 113310 (2003).
 - [10] T. Ando, T. Nakanishi, and R. Saito, J. Phys. Soc. Jpn. **67**, 2857 (1998).
 - [11] K. S. Novoselov *et al.*, Nature **438**, 197 (2005).
 - [12] S. V. Morozov *et al.*, Phys. Rev. Lett. **100**, 016602 (2008).
 - [13] J. H. Chen *et al.*, Nature Nanotechnology **3**, 206 (2008).
 - [14] T. Stauber, N. M. R. Peres, and F. Guinea, Phys. Rev. B **76**, 205423 (2007); E. H. Hwang and S. Das Sarma, Phys. Rev. B **77**, 115449 (2008).
 - [15] H.-P. Wittmann and A. Schmid, J. Low Temp. Phys. **69**, 131 (1987); Y. Y. Proskuryakov *et al.*, Phys. Rev. Lett. **86**, 4895 (2001); K. E. J. Goh, M. Y. Simmons, and A. R. Hamilton, Phys. Rev. B **77**, 235410 (2008).
 - [16] Y. Zhang *et al.*, Phys. Rev. Lett. **96**, 136806 (2006).
 - [17] N. N. Klimov *et al.*, Phys. Rev. B **78**, 195308 (2008).
 - [18] M. Yu. Kharitonov and K. B. Efetov, Phys. Rev. B **78**, 033404 (2008); K. Kechedzhi, O. Kashuba, and V. I. Fal'ko, Phys. Rev. B **77**, 193403 (2008).
 - [19] Unlike in usual 2DEGs, the current operator in graphene is momentum-independent, which requires renormalizations of the two current vertices in the conductivity diagram [3, 4].
 - [20] M. Polini *et al.*, Solid State Commun. **143**, 58 (2007).